

# Electronic Structure of Alkoxychromium(0) Carbene Complexes: A Joint TD-DFT/Experimental Study

Marta L. Lage, Israel Fernández,\* María J. Mancheño, and Miguel A. Sierra\*

Departamento de Química Orgánica, Facultad de Química, Universidad Complutense, 28040-Madrid, Spain

Received January 30, 2008

The joint computational (TD-DFT) experimental study of the UV–vis spectroscopy of alkoxychromium(0) carbene complexes accurately assigns the vertical transitions responsible for the observed spectra of these compounds. Both the LF and the MLCT band have a remarkably  $\pi-\pi^*$  character, which has been demonstrated by the strong dependence of the absorptions with the donor/acceptor nature of the substituent in *p*-substituted styrylchromium(0) carbene complexes. The effect of the substituent is also related with the equilibrium geometry of the complexes and the occupations of the *p* atomic orbital of the carbene carbon atom. Additionally, the ferrocenyl moiety behaves in chromium(0) (Fischer) carbene complexes as a  $\pi$ -donor group.

## Introduction

The organometallic photochemistry of chromium(0)carbene complexes is, perhaps, one of the few metal-mediated photoreactions of general application in organic synthesis.<sup>1</sup> The photogeneration of ketenes from chromium(0)carbene and its reaction with ketenophiles led to many different ketene-derived products.<sup>1a</sup> Recently, we opened new photochemical noncarbonylative reaction pathways, including type I stepwise photodiotropies and  $\alpha$ - fragmentations to the carbene ligand.<sup>2</sup> Simultaneously, we have thoroughly studied the mechanism of the photocarbonylation, which involves the excitation to the  $S_1$  state followed by a fast ISC (intersystem crossing) to a  $T_1$  state with a metallacyclopro-

panone structure.<sup>3</sup> During these and related studies, we became aware that the electronic structure of Fischer carbene complexes has been scarcely studied.

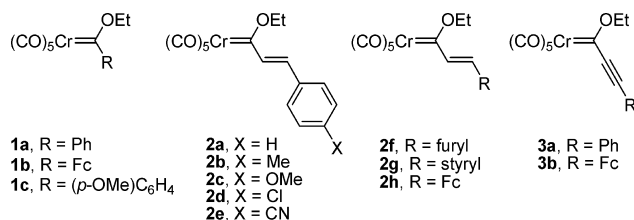
Chromium(0) carbene complexes are strongly colored compounds, their color ranging from pale yellow to dark red. The UV–vis spectra of Fischer metal–carbene complexes shows three well-defined absorptions: a spin-forbidden metal–ligand charge transfer (MLCT) absorption around 500 nm, the spin-allowed and moderately intense LF absorption in the range of 350–450 nm, and one additional ligand-field (LF) transition in the range of 300–350 nm.<sup>1a</sup> There is a lower energy LF transition usually masked by the intense MLCT absorption, although it has been observed in the non-heteroatom-stabilized carbene complex  $(CO)_5W=CPh(p\text{-MeOPh})$ .<sup>4</sup> On the basis of very early molecular orbital calculations,<sup>5</sup> the MLCT band has been assigned to the promotion of an electron from the nonbonding metal-centered

\* To whom correspondence should be addressed. E-mail: israel@quim.ucm.es (I.F.), sierraor@quim.ucm.es (M.A.S.).

(1) Reviews in the photochemistry of Fischer carbene complexes: (a) Hegedus, L. S. *Tetrahedron* **1997**, *53*, 4105. (b) Schwindt, M. A.; Miller, J. R.; Hegedus, L. S. *J. Organomet. Chem.* **1991**, *413*, 143. (c) Hegedus, L. S. *Comprehensive Organometallic Chemistry II*; Abel, E. W., Stone, F. G. A., Wilkinson, G., Eds.; Pergamon: Oxford, 1995; vol. 12, p 549. Selected reviews in the chemistry and synthetic application of Fischer carbene complexes. (d) Dötz, K. H.; Fischer, H.; Hofmann, P.; Kreissel, R.; Schubert, U.; Weiss, K. *Transition Metal Carbene Complexes*; Verlag Chemie: Deerfield Beach, FL, 1983. (e) Wulff, W. D. *Comprehensive Organometallic Chemistry II*; Abel, E. W., Stone, F. G. A., Wilkinson, G., Eds.; Pergamon: Oxford, U.K., 1995; Vol. 12, p 470. (f) Harvey, D. F.; Sigano, D. M. *Chem. Rev.* **1996**, *96*, 271. (g) Aumann, R.; Nienaber, H. *Adv. Organomet. Chem.* **1997**, *41*, 163. (h) Sierra, M. A. *Chem. Rev.* **2000**, *100*, 3591. (i) de Meijere, A.; Schirmer, H.; Duetsch, M. *Angew. Chem., Int. Ed.* **2000**, *39*, 3964. (j) Barluenga, J.; Santamaría, J.; Tomás, M. *Chem. Rev.* **2004**, *104*, 2259. (q) Gómez-Gallego, M.; Mancheño, M. J.; Sierra, M. A. *Acc. Chem. Res.* **2005**, *38*, 44. (k) Sierra, M. A.; Gómez-Gallego, M.; Martínez-Álvarez, R. *Chem.—Eur. J.* **2007**, *13*, 736–2.

(2) (a) Arrieta, A.; Cossío, F. P.; Fernández, I.; Gómez-Gallego, M.; Lecea, B.; Mancheño, M. J.; Sierra, M. A. *J. Am. Chem. Soc.* **2000**, *122*, 11509. (b) Sierra, M. A.; Fernández, I.; Mancheño, M. J.; Gómez-Gallego, M.; Torres, M. R.; Cossío, F. P.; Arrieta, A.; Lecea, B.; Poveda, A.; Jiménez-Barbero, J. *J. Am. Chem. Soc.* **2003**, *125*, 9572. (c) Fernández, I.; Sierra, M. A.; Gómez-Gallego, M.; Mancheño, M. J.; Cossío, F. P. *Angew. Chem., Int. Ed.* **2006**, *45*, 125. (3) Fernández, I.; Sierra, M. A.; Mancheño, M. J.; Gómez-Gallego, M.; Cossío, F. P. *Chem.—Eur. J.* **2005**, *11*, 5988. (4) Fong, L. K.; Cooper, N. J. *J. Am. Chem. Soc.* **1984**, *106*, 2595. (5) (a) Block, T. J.; Fenske, R. F.; Casey, C. P. *J. Am. Chem. Soc.* **1976**, *98*, 441. (b) Nakatsuji, H.; Uskio, J.; Yonezawa, T. *J. Am. Chem. Soc.* **1983**, *105*, 426. (c) Foley, H. C.; Strubinger, L. M.; Targos, T. S.; Geoffroy, G. L. *J. Am. Chem. Soc.* **1983**, *105*, 3064. (6) Fischer, E. O.; Maasböl, A. *J. Organomet. Chem.* **1968**, *12*, P15–P17.

Chart 1



orbital HOMO to the carbene-carbon p-orbital-centered LUMO, whereas the LF band is attributed to the more energetic population of the metal-centered LUMO+1.

The strong dependence of the position of the bands with the substitution on the carbene carbon atom is evident. For example, chromium(0)amino carbene complexes, amino groups being strong  $\pi$  donors, are in general pale-yellow compounds, whereas chromium(0)alkoxy carbene complexes, alkoxy groups being softer donors than amino groups, are deep-yellow complexes. Analogously, the substitution of a Me group by a  $\pi$ -acceptor substituent (e.g., Ph- or Ph-CHCH-) results in a strong red-shift, and the complexes are deep red. To fully understand the photochemistry and other electronic properties of these compounds, we undertook a joint experimental and computational study to accurately assign the observed transitions in the UV-vis spectra of alkoxychromium(0) (Fischer) carbene complexes, the effect of substituents attached to the carbene ligand on the electronic structure, and the equilibrium geometries of these compounds. The study includes ferrocenyl-substituted complexes to check the effect of an additional metal atom on the electronic properties of Fischer carbenes. Reported in this article are the results of this study, which change the interpretation of the UV-vis spectroscopy of these complexes and disclose a novel two-electron stabilizing interaction between proximate metal centers.

## Experimental Section

**General Procedures.** Aryl and alkynyl **1** and **3** were prepared following the standard alkyllithium addition-alkylation sequence reported by Fischer,<sup>6</sup> whereas styryl **2** were prepared from the pentacarbonyl(ethoxy)methyl-chromium(0) carbene complex and the corresponding benzaldehyde following the standard Aumann reaction.<sup>7</sup> The structures of all compounds were established by NMR experiments and by comparison with the analytical data reported for **1a**,<sup>8a</sup> **1b**,<sup>8b</sup> **1c**,<sup>8c</sup> **2a**,<sup>7</sup> **2b**,<sup>9a</sup> **2c**,<sup>9a</sup> **2d**,<sup>9a</sup> **2e**,<sup>9a</sup> **2f**,<sup>8c</sup> **2g**,<sup>8c</sup> **2h**,<sup>9b</sup> **3a**,<sup>10a</sup> and **3b**<sup>10b</sup> (Chart 1). All reactions were carried out under argon atmosphere, and all solvents used in this work were purified by distillation and were freshly distilled immediately before use. Tetrahydrofuran (THF) and diethylether were distilled from

sodium/benzophenone and dichloromethane (DCM) from calcium hydride. Flame-dried glassware and standard Schlenk techniques were used for moisture-sensitive reactions. Silica gel for flash column chromatography purification of crude mixtures was purchased from Merck (230–400 mesh), and the identification of products was made by thin-layer chromatography kieselgel 60F-254. UV light ( $\lambda = 254$  nm) and 5% phosphomolybdic acid solution in 95% EtOH were used to develop the plates. NMR spectra were recorded at 22 °C in CDCl<sub>3</sub> on Bruker Avance 300 (300 MHz for <sup>1</sup>H, 75 MHz for <sup>13</sup>C) or Bruker AM-500 (500 MHz for <sup>1</sup>H, 125 MHz for <sup>13</sup>C). IR spectra were taken on a Bruker Tensor 27 (MIR 8000–400 cm<sup>-1</sup>) spectrometer in CHCl<sub>3</sub> solution. UV measures were recorded on a Varian (Cary 50) spectrometer. All commercially available products were used without further purification.

**Computational Details.** All of the calculations reported in this paper were obtained with the GAUSSIAN 03 suite of programs.<sup>11</sup> Electron correlation was partially taken into account using the hybrid functional usually denoted as B3LYP<sup>12</sup> using the double- $\xi$  quality plus polarization def2-SVP basis set for all atoms.<sup>13</sup> Calculation of the vibrational frequencies<sup>14</sup> at the optimized geometries showed that the compounds are minima on the potential-energy surface. Calculations of absorption spectra were accomplished in the present work using the time-dependent density functional theory (TD-DFT)<sup>15</sup> method at the same level. The assignment of the excitation energies to the experimental bands was performed on the basis of the energy values and oscillator strengths. The B3LYP Hamiltonian was chosen because it was proven to provide accurate structures and reasonable UV-vis spectra for a variety of chromophores<sup>16</sup> including organometallic complexes.<sup>17</sup>

The atomic orbital occupations and donor-acceptor interactions have been computed using the natural bond orbital (NBO) method.<sup>18</sup> The energies associated with these two-electron interactions have been computed according to the following equation,

$$\Delta E_{\varphi\varphi^*}^{(2)} = -n_{\varphi} \frac{\langle \varphi^* | \hat{F} | \varphi \rangle^2}{\varepsilon_{\varphi^*} - \varepsilon_{\varphi}} \quad (1)$$

where  $F$  is the DFT equivalent of the Fock operator and  $\varphi$  and  $\varphi^*$  are two filled and unfilled NBOs having  $\varepsilon_{\varphi}$  and  $\varepsilon_{\varphi^*}$  energies,

- (7) Aumann, R.; Heinen, H. *Chem. Ber.* **1987**, *120*, 537.  
(8) (a) Fischer, E. O.; Dötz, K. H. *J. Organomet. Chem.* **1972**, *36*, C4. (b) Dötz, K. H.; Dietz, R.; Neugebauer, D. *Chem. Ber.* **1979**, *112*, 1486. (c) Connor, J. A.; Rose, P. D.; Turner, R. M. *J. Organomet. Chem.* **1973**, *55*, 111.  
(9) (a) Gómez-Gallego, M.; Mancheño, M. J.; Ramírez, P.; Piñar, C.; Sierra, M. A. *Tetrahedron* **2000**, *56*, 4893. (b) Jayaprakash, K. N.; Ray, P. C.; Matsuoka, I.; Bhadbhade, M. M.; Puranik, V. G.; Das, P. K.; Nishihara, H.; Sarkar, A. *Organometallics* **1999**, *18*, 3851.  
(10) (a) Aumann, R.; Hinterding, P. *Chem. Ber.* **1993**, *126*, 421. (b) Sierra, M. A.; Mancheño, M. J.; Del Amo, J. C.; Fernández, I.; Gómez-Gallego, M.; Torres, M. R. *Organometallics* **2003**, *22*, 384.

- (11) Frisch, M. J.; Trucks, G. W.; Schlegel, H. B.; Scuseria, G. E.; Robb, M. A.; Cheeseman, J. R.; Montgomery, J. A., Jr.; Vreven, T.; Kudin, K. N.; Burant, J. C.; Millam, J. M.; Iyengar, S. S.; Tomasi, J.; Barone, V.; Mennucci, B.; Cossi, M.; Scalmani, G.; Rega, N.; Petersson, G. A.; Nakatsuji, H.; Hada, M.; Ehara, M.; Toyota, K.; Fukuda, R.; Hasegawa, J.; Ishida, M.; Nakajima, T.; Honda, Y.; Kitao, O.; Nakai, H.; Klene, M.; Li, X.; Knox, J. E.; Hratchian, H. P.; Cross, J. B.; Bakken, V.; Adamo, C.; Jaramillo, J.; Gomperts, R.; Stratmann, R. E.; Yazyev, O.; Austin, A. J.; Cammi, R.; Pomelli, C.; Ochterski, J. W.; Ayala, P. Y.; Morokuma, K.; Voth, G. A.; Salvador, P.; Dannenberg, J. J.; Zakrzewski, V. G.; Dapprich, S.; Daniels, A. D.; Strain, M. C.; Farkas, O.; Malick, D. K.; Rabuck, A. D.; Raghavachari, K.; Foresman, J. B.; Ortiz, J. V.; Cui, Q.; Baboul, A. G.; Clifford, S.; Cioslowski, J.; Stefanov, B. B.; Liu, G.; Liashenko, A.; Piskorz, P.; Komaromi, I.; Martin, R. L.; Fox, D. J.; Keith, T.; Al-Laham, M. A.; Peng, C. Y.; Nanayakkara, A.; Challacombe, M.; Gill, P. M. W.; Johnson, B.; Chen, W.; Wong, M. W.; Gonzalez, C.; Pople, J. A. *Gaussian 03*, revision C.02; Gaussian, Inc.: Wallingford, CT, 2004.  
(12) (a) Becke, A. D. *J. Chem. Phys.* **1993**, *98*, 5648. (b) Lee, C.; Yang, W.; Parr, R. G. *Phys. Rev. B* **1998**, *37*, 785. (c) Vosko, S. H.; Wilk, L.; Nusair, M. *Can. J. Phys.* **1980**, *58*, 1200.  
(13) Weigend, F.; Alrichs, R. *Phys. Chem. Chem. Phys.* **2005**, *7*, 3297.  
(14) McIver, J. W.; Komornicki, A. K. *J. Am. Chem. Soc.* **1972**, *94*, 2625.  
(15) (a) Casida, M. E. *Recent Developments and Applications of Modern Density Functional Theory*; Elsevier: Amsterdam, 1996; Vol. 4. (b) Casida, M. E.; Chong, D. P. *Recent Advances in Density Functional Methods*; World Scientific: Singapore, 1995; Vol. 1, p 155.  
(16) For a review, see: (a) Dreuw, A.; Head-Gordon, M. *Chem. Rev.* **2005**, *105*, 4009.

**Table 1.** Comparison of Main UV–vis Excitation Energies ( $\lambda_{\text{max}}$  in nm), Oscillator Strengths ( $f$ , in Parentheses), Calculated Bond Distances (in Å) and (NBO)p occupation for **1–3**

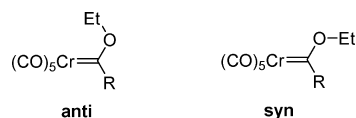
entry	complex	$\lambda_1$ (LF band) <sup>a</sup>	$\lambda_2$ (MLCT band) <sup>a</sup>	C–C bond length <sup>b</sup>	Cr–C bond length <sup>b</sup>	p occupation <sup>b</sup>
1	<b>1a</b>		406 (387, 0.177)		2.084	0.584
2	<b>1b</b>		418 (380.7, 0.183)		2.101	0.604
3	<b>1c</b>		426 (400, 0.222)		2.107	0.595
4	<b>2a</b>	323 (320, 0.529)	471 (450, 0.358)	1.468	2.074	0.627
5	<b>2b</b>	337 (328, 0.596)	468 (449, 0.405)	1.466	2.078	0.627
6	<b>2c</b>	357 (343, 0.583)	468 (449, 0.476)	1.463	2.083	0.630
7	<b>2d</b>	330 (332, 0.591)	472 (456, 0.403)	1.469	2.072	0.628
8	<b>2e</b>	307 (328, 0.656)	481 (478, 0.384)	1.473	2.064	0.629
9	<b>2f</b>	355 (332, 0.551)	479 (456, 0.372)	1.463	2.076	0.635
10	<b>2g</b>	360 (360, 0.842)	484 (481, 0.555)	1.462	2.078	0.633
11	<b>2h</b>	333 (330, 0.202)	465 (438, 0.133)	1.460	2.086	0.629
12	<b>3a</b>	281 (304, 0.339)	504 (472, 0.292)	1.413	2.024	0.678
13	<b>3b</b>	306 (303, 0.118)	500 (453, 0.255)	1.408	2.041	0.678

<sup>a</sup> The first value corresponds to experimental data (recorded at room temperature in hexane with a concentration ca.  $1 \times 10^{-5}$  mol/L). In parenthesis, the first value corresponds to the computed TD-B3LYP/def2-SVP gas-phase vertical excitation energies, and the second one is the corresponding oscillator strength. <sup>b</sup> All data have been computed at the B3LYP/def2-SVP level.

respectively;  $n\sigma$  stands for the occupation number of the filled orbital.

Geometry optimizations (B3LYP/def2-SVP) were carried out starting with the anti form (an orientation where the methyl group of the ethoxy substituent is directed toward the metal fragment) of aryl- and styryl-metal(0) Fischer carbene **1** and **2** respectively, whereas the syn form was selected in the case of alkynyl-substituted carbenes **3**. These species are the most stable isomers in the gas phase and in the solid state.<sup>19</sup>

#### Chart 2



## Results and Discussion

The suitability of selected TD-B3LYP/def2-SVP (gas phase) method to accomplish the objectives of this work was checked first. Data gathered in Table 1, which includes the calculated oscillator strengths of the main absorptions, show a good agreement between the calculated vertical excitation energies and the wavelengths of the absorption maxima in the experimental UV–vis spectra. This correlation allows to the accurate assignment of the experimentally observed bands for the specific transitions discussed below.

The effect of the introduction of a  $\pi$  bridge in the carbon substituent attached to the carbene ligand in the electronic structure of chromium(0)alkoxy carbenes was studied comparing **1a**, **2a**, and **3a**, which have a phenyl, styryl, and phenylethynyl group, respectively. The UV spectrum of the

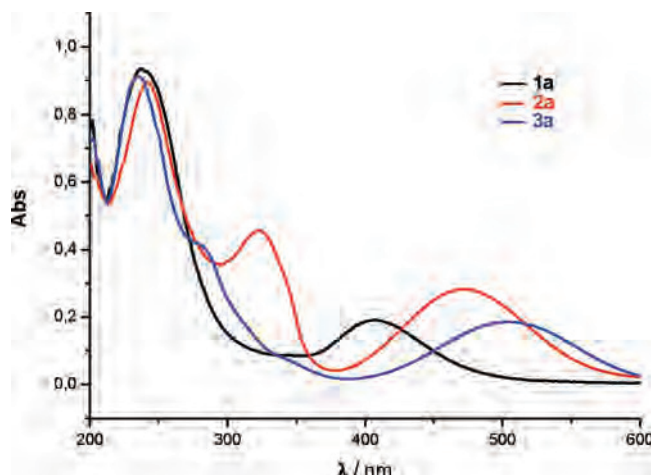


**Figure 1.** Room-temperature UV–vis spectra of **1a**, **2a**, and **3a** in hexane (in all cases the concentration of sample is ca.  $1 \times 10^{-5}$  mol/L).

Ph-substituted carbene **1a** shows two different absorptions (at 239 and 406 nm), whereas styryl and phenylethynyl **2a** and **3a** present three bands, with the new absorption located at ca. 323 and 281 nm, respectively (Figure 1).

TD-DFT calculations show appealing differences with respect to earlier work.<sup>5</sup> Previously, the MLCT band was attributed to the HOMO  $\rightarrow$  LUMO transition. However, the TD-DFT data ascribe in all cases the MLCT band (in the range of 400–500 nm) to the promotion of one electron from the metal-centered HOMO-1 to the LUMO, which is a  $\pi$ -extended orbital involving the p atomic orbital of the carbene carbon atom (Figure 2). The presence of a  $\pi$  link between the phenyl group and the metal moiety (**2a**, **3a**) provokes, as expected, a strong red-shift of this absorption (406 nm for **1a** compared to 471 and 500 nm for **2a** and **3a**, respectively). The additional band of **2a** and **3a** (300–350 nm) is assigned on the basis of the TD-DFT calculations to the LF transition from the HOMO-3 (centered in the  $\pi$  system of the carbene ligand, Figure 2) to the LUMO. The latter absorption is blue-shifted in **3a** compared to **2a**, whereas the MLCT is red-shifted in **3a** respect **2a**. Interestingly, the NBO occupation of the p atomic orbital of the carbene carbon is clearly increased in the ethynyl-substituted carbene **3a** (0.678) compared to **2a** (0.604, entries 2 and 12, Table 1), which nicely agrees with the recently reported

- (17) Recent examples:(a) Andzelm, J.; Rawlett, A. M.; Orlicki, J. A.; Snyder, J. F. *J. Chem. Theory Comput.* **2007**, *3*, 870–877. (b) Nemykin, V. N.; Makarova, E. A.; Grosland, J. O.; Hadt, R. G.; Kopolov, A. Y. *Inorg. Chem.* **2007**, *46*, 9591. (c) Santi, S.; Orian, L.; Donoli, A.; Durante, C.; Bisello, A.; Ganis, P.; Ceccon, A.; Crociani, L.; Benetollo, F. *Organometallics* **2007**, *26*, 5867.
- (18) (a) Foster, J. P.; Weinhold, F. *J. Am. Chem. Soc.* **1980**, *102*, 7211. (b) Reed, A. E.; Weinhold, F. *J. Chem. Phys.* **1985**, *83*, 1736. (c) Reed, A. E.; Weinstock, R. B.; Weinhold, F. *J. Chem. Phys.* **1985**, *83*, 735. (d) Reed, A. E.; Curtiss, L. A.; Weinhold, F. *Chem. Rev.* **1988**, *88*, 899.
- (19) (a) Fernández, I.; Cossío, F. P.; Arrieta, A.; Lecea, B.; Mancheño, M. J.; Sierra, M. A. *Organometallics* **2004**, *23*, 1065. (b) Andrada, D. M.; Zoloff Michoff, M. E.; Fernández, I.; Granados, A. M.; Sierra, M. A. *Organometallics* **2007**, *26*, 5854.



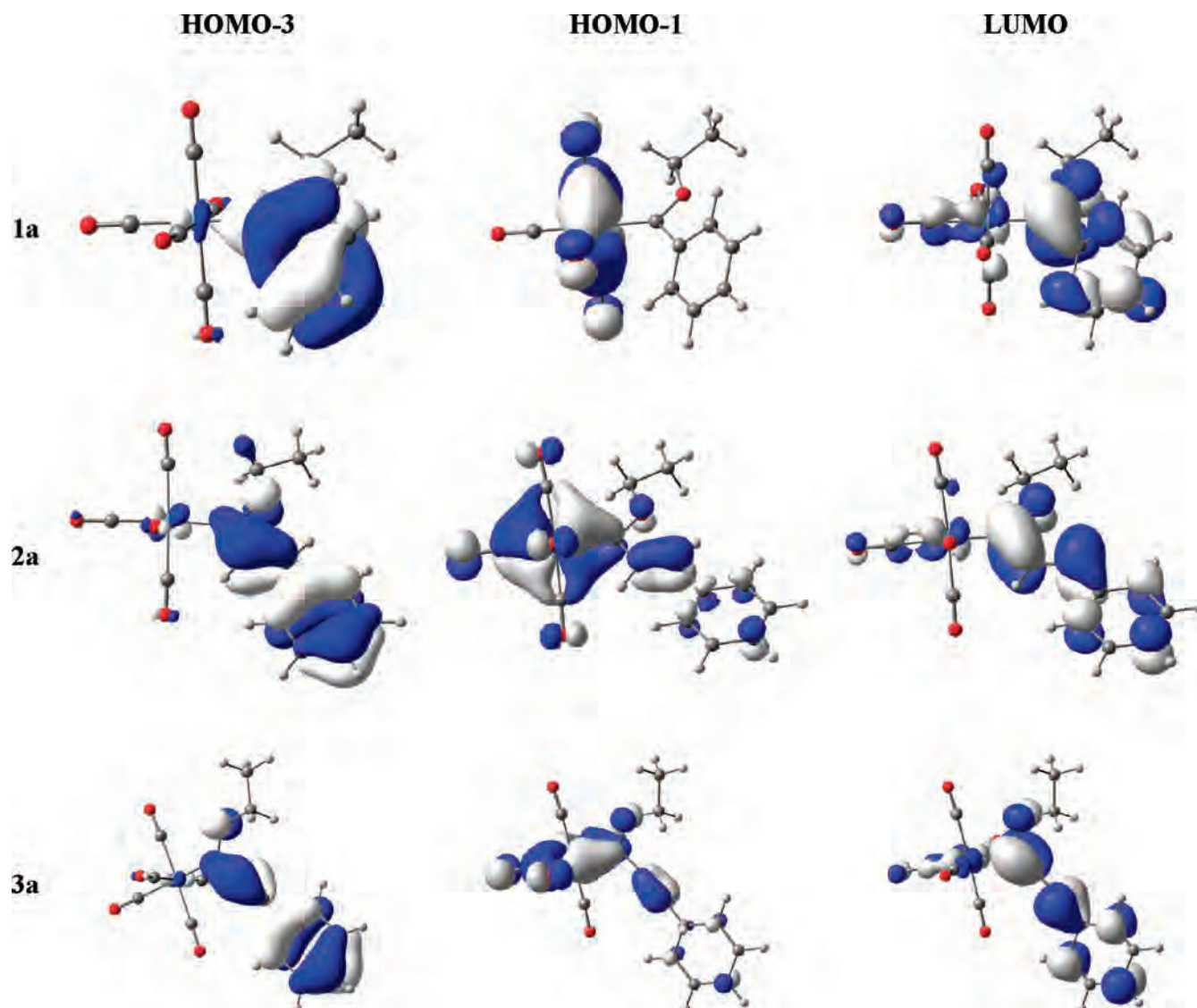


**Figure 2.** Molecular orbitals of **1a**, **2a**, and **3a** calculated at the B3LYP/def2-SVP level (isosurface value of 0.035).

**Table 2.** Room Temperature UV–vis Spectra of **1a**, **2a**, and **3a** in Different Solvents

entry	complex	$\lambda_1$ (LF band) <sup>a</sup>	$\lambda_2$ (MLCT band) <sup>a</sup>
1	<b>1a</b>		406, 387, <b>396</b>
2	<b>2a</b>	323, 325, <b>324</b>	471, 464, <b>458</b>
3	<b>3a</b>	281, 281, <b>281</b>	504, 496, <b>489</b>

<sup>a</sup> The first value (plain) corresponds to hexane, the second (italics) to dichloromethane, and the third (bold) to acetonitrile.

finding of the higher  $\pi$ -conjugative ability of triple bonds compared with double bonds.<sup>20</sup>

The predominant  $\pi$ - $\pi^*$  character of the LF transition should be reflected in a small solvatochromism.<sup>17b</sup> Thus, we performed UV–vis spectra in solvents with different polarity. Data in Table 2 show that the LF band of planar **2a** and **3a**, which involves genuine  $\pi$  orbitals, is independent of the polarity of the solvent. This result confirms the  $\pi$ - $\pi^*$  nature of this absorption. As expected, we observed a small solvatochromic effect (ca. 7–13 nm) in the absorption, which

is in excellent agreement with the MLCT nature of this transition.<sup>17b</sup>

The effect of  $\pi$  substituents attached to the aryl group in styryl complexes on the position of the different UV–vis bands was studied next. A series of styryl-substituted complexes **2a–g** was prepared to cover a representative range of compounds including  $\pi$ -donor and  $\pi$ -electron withdrawing groups. Figure 3 compiles the UV spectra of these compounds. As predicted, the position of the MLCT band is slightly dependent on the nature of the p-substituent of the phenyl group (ranging from 468 nm for the strongly donating MeO group to 481 nm for the CN acceptor group), whereas the LF transition strongly depends on this substitution (357 nm for the MeO group to 307 nm for the CN group). Thus,  $\pi$ -donor substituents attached to the phenyl group lead to red-shifts of the LF band while having almost no effect on the MLCT band.  $\pi$ -acceptor groups provoke significant blue-shifts in the LF band and small red shifts on the MLCT transition. This effect of substituents on the absorption of the complexes can be quantified by using the Hammett–Brown substituent constants<sup>21</sup> ( $\sigma_p^+$  or  $\sigma_p^-$ ) to

(20) (a) Cappel, D.; Tüllmann, S.; Krapp, A.; Frenking, G. *Angew. Chem., Int. Ed.* **2005**, *44*, 361. (b) Fernández, I.; Frenking, G. *Chem.–Eur. J.* **2006**, *12*, 3617.

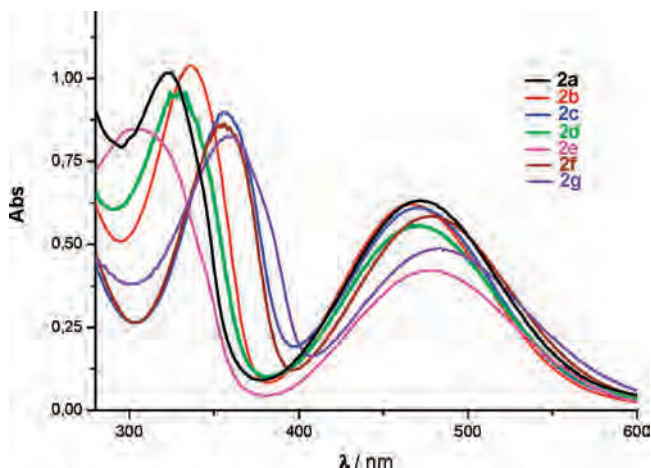


**Figure 3.** Room-temperature UV-vis spectra of **2a–g** in hexane (in all cases the concentration of sample is ca.  $1 \times 10^{-5}$  mol/L).

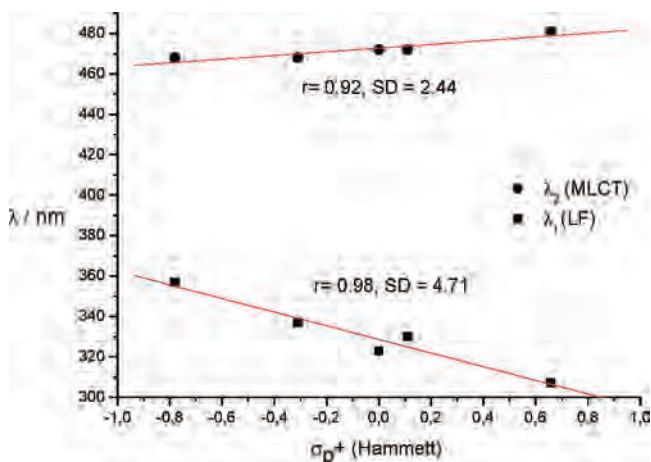
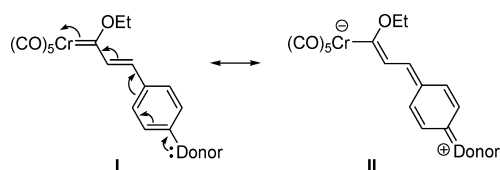


**Figure 4.** Plot of the wavelengths of absorption maxima of the LF band (squares) and MLCT band (circles) versus the  $\sigma_p^+$  values for **2a–e**.

#### Scheme 1



estimate the *through-resonance effect* (which means direct conjugation between the  $\pi$  group and the reaction center).<sup>22</sup> Very good to good linear relationships were found between the value of wavelengths of the absorption maxima and Hammett–Brown parameters for both bands (Figure 4, LF band: correlation coefficient 0.98 and standard error 4.71; MLCT band: correlation coefficient 0.92 and standard error 2.44). The higher slope of the linear correlation for the LF band provides additional support for the higher sensitivity of this absorption to the  $\pi$  conjugation compared to the MLCT band.

(21) (a) Okamoto, Y.; Brown, H. C. *J. Org. Chem.* **1957**, *22*, 485. (b) Stock, L. M.; Brown, H. C. *Adv. Phys. Org. Chem.* **1963**, *1*, 35.  $\sigma_p^+$  values taken from: (c) Hansch, C.; Leo, A. *Exploring QSAR. Fundamentals and Applications in Chemistry and Biology*, ACS Professional Reference Book, American Chemical Society: Washington, DC, 1995.

(22) Fernández, I.; Frenking, G. *J. Org. Chem.* **2006**, *71*, 2251, and references therein.

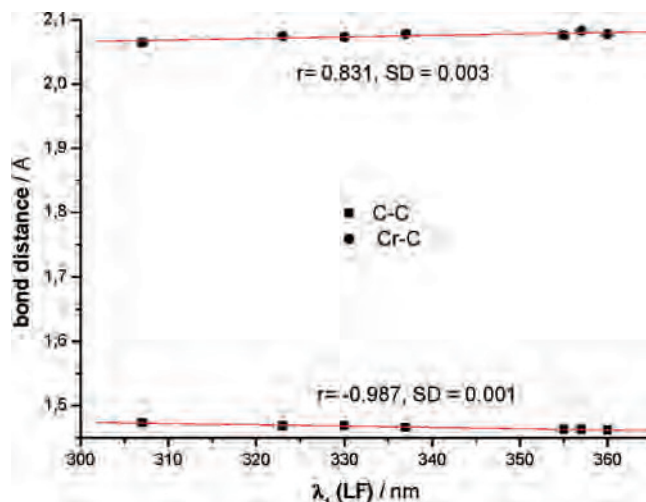


**Figure 5.** Plot of the wavelengths of absorption maxima of the LF band versus the C–C bond (squares) and Cr–C bond (circles) lengths for **2a–g**.

The effect of substituents other than phenyl groups directly attached to the C=C double bond of the carbene ligand was addressed next. Data in Figure 3 and Table 1 clearly show that furyl and  $\pi$ -extended styryl substituents (**2f** and **2g**, respectively) lead to strong bathochromic shifts of the LF absorption and smaller but significant red-shifts in the MLCT band compared to the reference **2a**. Similarly to the other styryl **2**, the TD-DFT calculations assign, in **2f** and **2g**, the LF band to the HOMO-3  $\rightarrow$  LUMO transition, whereas the MLCT is ascribed to the HOMO-1  $\rightarrow$  LUMO transition, analogously to the other **2** studied. Therefore, we can conclude that the origin of the absorptions is independent of the nature of the  $\pi$  link attached to the carbene carbon atom.

The effect of  $\pi$  substituents on the electronic structure of styryl-substituted Fischer carbene complexes translates in appreciable changes in the equilibrium geometry of the different compounds. In fact,  $\pi$ -donor substituents populate the resonance structure II (Scheme 1) and therefore shorten the C=C bond with the concomitant lengthening of the Cr=C bond (1.468 Å in **2a** to 1.463 Å in **2c** for the C=C bond, whereas the distance of the Cr=C bond increases from 2.074 Å in **2a** to 2.082 in **2c**, Table 1). As expected, strong acceptor substituents like a cyano group (**2e**) have the opposite effect in the bond distances because the resonance form II in Scheme 1 cannot be populated. Thus, electron-withdrawing groups provoke a lengthening of the C=C bond (from 1.468 Å in **2a** to 1.473 in the CN-substituted **2e**), whereas the distance of the Cr=C bond shortens from 2.074 Å in **2a** to 2.064 Å in **2e** (Table 1). Obviously, these geometrical features correlate with the position of the absorption maxima of the LF band, which as discussed above has the strongest dependence with the  $\pi$  conjugation. Again, very good linear relationships have been found between the latter geometrical features and the wavelengths of the LF absorption maxima (Figure 5, C–C bond length vs  $\lambda_1(\text{LF})$ : correlation coefficient 0.987 and standard error 0.001; Cr=C bond length vs  $\lambda_1(\text{LF})$ : correlation coefficient 0.831 and standard error 0.003). On the contrary, poorer linear cor-



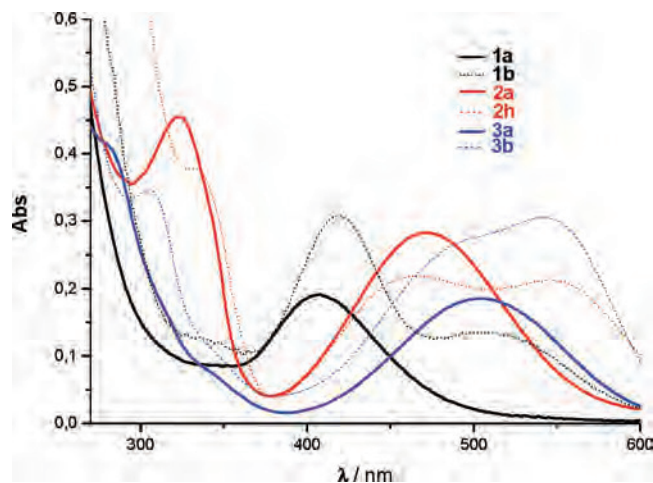


**Figure 6.** Room-temperature UV–vis spectra of **1a,b**, **2a,h**, and **3a,b** in hexane (in all cases the concentration of sample is ca.  $1 \times 10^{-5}$  mol/L).

relations between the bond lengths and the position of the absorption maxima of the MLCT band were found. This fact provides further support for the above mentioned higher sensitivity of the LF transition with the  $\pi$  conjugation compared to the MLCT band.

The effect of the presence of an additional metal center susceptible of interacting with the chromium carbene on the electronic structure of these complexes was finally addressed. Ph-substituted **1a**, **2a**, and **3a** were compared with their ferrocenyl analogues **1b**, **2h**, and **3b**, respectively (Figure 6 and Table 1). **2h** and **3b** bearing the ferrocenyl moiety experience slight blue-shifts in the MLCT band (except for **1b**, which experiences a slight red-shift) and a more pronounced red-shift in the LF band. This behavior is quite similar to the effect of a  $\pi$ -donor substituent attached to the p-position of the aryl groups of styrylchromium complexes (Figure 3). Moreover, the ferrocenyl group in **2h** and **3b** also leads to a shortening of the C=C bond and a lengthening of the Cr=C bond (entries 11 and 13, Table 1) compared to corresponding phenyl-substituted **2a** and **3a** (entries 4 and 12, Table 1), whereas the occupation of the p carbene orbital show only negligible changes by the presence of the ferrocenyl moiety compared to the analogous aryl derivatives. Therefore, we can conclude that the ferrocenyl group acts in chromium(0) carbene complexes as a  $\pi$ -donor substituent.

As stated above, the MLCT band of ferrocene derivative **1b** is slightly red-shifted compared to the phenyl-substituted **1a**. Comparison between the wavelength of the MLCT-absorption maxima of **1a** and its p-MeO derivative **1c**, which is also red-shifted, solves this apparent contradiction and demonstrates that the ferrocenyl moiety behaves as a  $\pi$ -donor substituent.<sup>23</sup> Additionally, the origins of this donation can

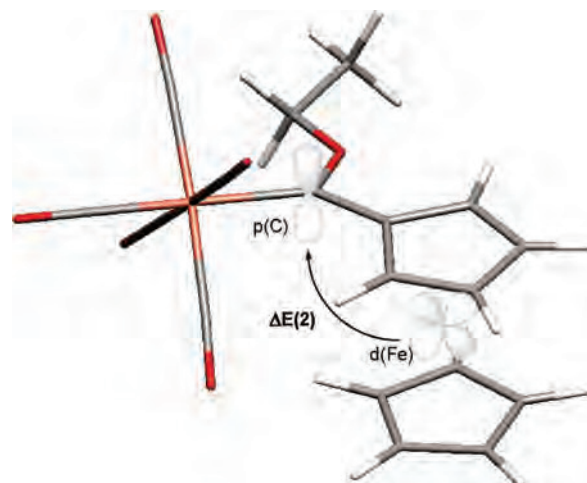


**Figure 7.** Two-electron interaction in **1b**.

be found with the help of the second-order perturbation theory of the NBO method.<sup>18</sup> A stabilizing two-electron interaction between the occupied d orbital of the iron atom and the p orbital of the carbene carbon atom (associated second-order perturbation energy ( $\Delta E^{(2)} = -0.60$  kcal/mol) was found (Figure 7).<sup>24</sup> This effect is very likely responsible for the computed higher p occupation in **1b** compared to that in **1a**.

## Conclusions

The joint computational (TD-DFT) experimental study of the UV–vis spectroscopy of alkoxychromium(0) carbene complexes accurately assign the vertical transitions, which are responsible for the observed spectra of these compounds. Both the LF and the MLCT band have a remarkable  $\pi$ – $\pi^*$  character, which has been demonstrated by the strong dependence of the absorptions with the donor/acceptor nature of the substituent in p-substituted styrylchromium(0) carbene complexes. The effect of the substituent is also related to the equilibrium geometry of the complexes and the occupations of the p atomic orbital of the carbene carbon atom. Additionally, the ferrocenyl moiety behaves in chromium(0) (Fischer) carbene complexes as a  $\pi$ -donor group. The application of these findings to the mechanistic and synthetic photochemistry of these complexes is now underway in our laboratories.

**Acknowledgment.** Support for this work under grants CTQ2007–67730-C02–01/BQU and CSD2007–0006 (Programa Consolider-Ingenio 2010) from the MEC (Spain) is gratefully acknowledged. M. L. Lage thanks the MEC (Spain) for a FPU fellowship. I. F. is a Ramón y Cajal fellow.

**Supporting Information Available:** Cartesian coordinates and total energies (noncorrected zero-point vibrational energies included) of all of the stationary points discussed in the text. This material is available free of charge via the Internet at <http://pubs.acs.org>.

IC800187R

(23) This result agrees with the reported  $\pi$ -donor nature of the ferrocenyl moiety. See: (a) Arnett, E. M.; Bushick, R. D. *J. Org. Chem.* **1962**, *27*, 111, and references therein.

(24) (a) An analogous albeit stronger interaction has been reported to occur between the iron atom and the p orbital of the boron atom in ferrocenylboranes and boroles, see: Bolte, M. J.; Bats, W.; Scheibitz, M.; Lerner, H.-W.; Nowik, I.; Herber, R. H.; Krapp, A.; Lein, M.; Holthausen, M. C.; Wagner, M. *Chem.–Eur. J.* **2005**, *11*, 584. (b) Braunschweig, H.; Fernández, I.; Frenking, G.; Kupfer, T. *Angew. Chem., Int. Ed.* **2008**, *47*, 1951.